Fitoterapia 125 (2018) 174–183

Contents lists available at ScienceDirect

Fitoterapia

journal homepage: www.elsevier.com/locate/fitote

7α,8α-Epoxynagilactones and their glucosides from the twigs of *Podocarpus nagi*: Isolation, structures, and cytotoxic activities

Yuan-Dong Zheng[a,b,c,d,1], Gang Bai[a,c,d,1], Chunping Tang[a,b], Chang-Qiang Ke[a,b], Sheng Yao[a,b], Lin-Jiang Tong[a,c], Fang Feng[a,c], Yan Li[a,c], Jian Ding[a,c,d], Hua Xie[a,c,*], Yang Ye[a,b,c,d,**]

[a] State Key Laboratory of Drug Research, Shanghai Institute of Materia Medica, Chinese Academy of Sciences, Shanghai 201203, People's Republic of China
[b] Natural Products Chemistry Department, Shanghai Institute of Materia Medica, Chinese Academy of Sciences, Shanghai 201203, People's Republic of China
[c] University of Chinese Academy of Sciences, Beijing 100049, People's Republic of China
[d] School of Life Science and Technology, Shanghai Tech University, Shanghai 201210, People's Republic of China

ARTICLE INFO

Keywords:
Podocarpus nagi
Type B nagilactone
Cytotoxic activity
Apoptosis

ABSTRACT

A phytochemical investigation of twigs of *Podocarpus nagi* resulted in the identification of eight new type B nagilactones (**1–8**), all bearing a 7α,8α-epoxy-9(11)-enolide substructure, along with two known analogs (**9–10**). Their structures were determined on the basis of spectroscopic analysis, including HRESIMS, IR and NMR experiments, and X-ray crystallographic analysis. *In vitro* cytotoxic assay exhibited that compounds **1**, **2**, **9** and **10** could induce antiproliferation against three different types of human cancer cells while compounds **3** and **5** were inactive. Notably, the IC_{50} value of compound **1** is 0.208 μM for A431 human epidermoid carcinoma cells, reaching the same level as the positive control combretastatin A-4 (0.104 μM). Furthermore, compound **1** performed a strong inhibition of cancer cells by triggering apoptosis and arresting the cell cycle at G_1 phase. These results unfold potential anticancer therapeutic applications of type B nagilactones.

1. Introduction

Cancer has been the leading cause of death and global health problems considering the poor survival rates and huge medical expenses. Continuing efforts have been taken on developing strategies for prevention, early diagnosis, and clinical treatment [1–2]. Natural products have long played an important role in new drug discovery, and continuously provided candidate compounds that have entered clinical trials or become clinical medicines, such as paclitaxel [3–4]. Nowadays, searching potential structures from nature sources is still one of the most important ways for contemporary pharmaceutical development [5–7].

Nagilactones (podolactones) are a class of structurally fascinating and synthetically challenging nature products. These nor- and bisnor-diterpenoid lactones feature a γ-lactone moiety between C-6 and C-19, and a δ-lactone moiety between C-12 and C-14 [8–10]. According to the conjugated lactone system of rings B and C, nagilactones are sorted into three types. Type A structure owns a α-pyrone [8(14), 9(11)-dienolide] fragment, type B has a 7α,8α-epoxy-9(11)-enolide moiety, and type C contains a 7(8), 9(11)-dienolide substructure [9,11–12]. Nagilactones exhibited a broad range of biological activities such as antiproliferative [13], insecticidal [14], antifungal [15], and cytotoxic [16–17] activity. Recently, nagilactone B, one of reported nagilactones, has been reported used as a liver X receptor transcriptional regulator to suppress atherosclerosis in apoE-deficient mice [18]. Type B nagilactones, have demonstrated strong cytotoxic activity against P388 murine leukemia cells [19], and inhibited phorbol ester TPA-induced activation of activator protein-1 activity, which may be valuable for the prevention and treatment of cancers [20]. Up to now, about 50 type B nagilactones were identified, mostly isolated from the genus *Podocarpus*[9,19].

Podocarpus nagi (Thunb) Zoll. et Mor ex Zoll is widely distributed in Japan and the southern part of China [21]. Its leaves and roots were used as folk medicine for the treatment of rheumatism and arthritis [22]. Our previous work revealed the existence of cyclopeptides and diterpenoids in this plant [23–25]. As a part of our continuous effort to seek bioactive compounds, an investigation of type B nagilactions from P. nagi was conducted.

As a result, a total of eight new (**1–8**) and two known (**9–10**) type B nagilactones have been identified (Chart 1). Their structures were characterized by extensive analysis of spectroscopic data. The cytotoxic

* Correspondence to: H. Xie, State Key Laboratory of Drug Research, Shanghai Institute of Materia Medica, Chinese Academy of Sciences, Shanghai 201203, People's Republic of China.
** Correspondence to: Y. Ye, Natural Products Chemistry Department, Shanghai Institute of Materia Medica, Chinese Academy of Sciences, Shanghai 201203, People's Republic of China.
E-mail addresses: hxie@simm.ac.cn (H. Xie), yye@mail.shcnc.ac.cn (Y. Ye).
[1] Both authors contributed equally to this study.

https://doi.org/10.1016/j.fitote.2018.01.007
Received 8 December 2017; Received in revised form 9 January 2018; Accepted 13 January 2018
0367-326X/ © 2018 Published by Elsevier B.V.

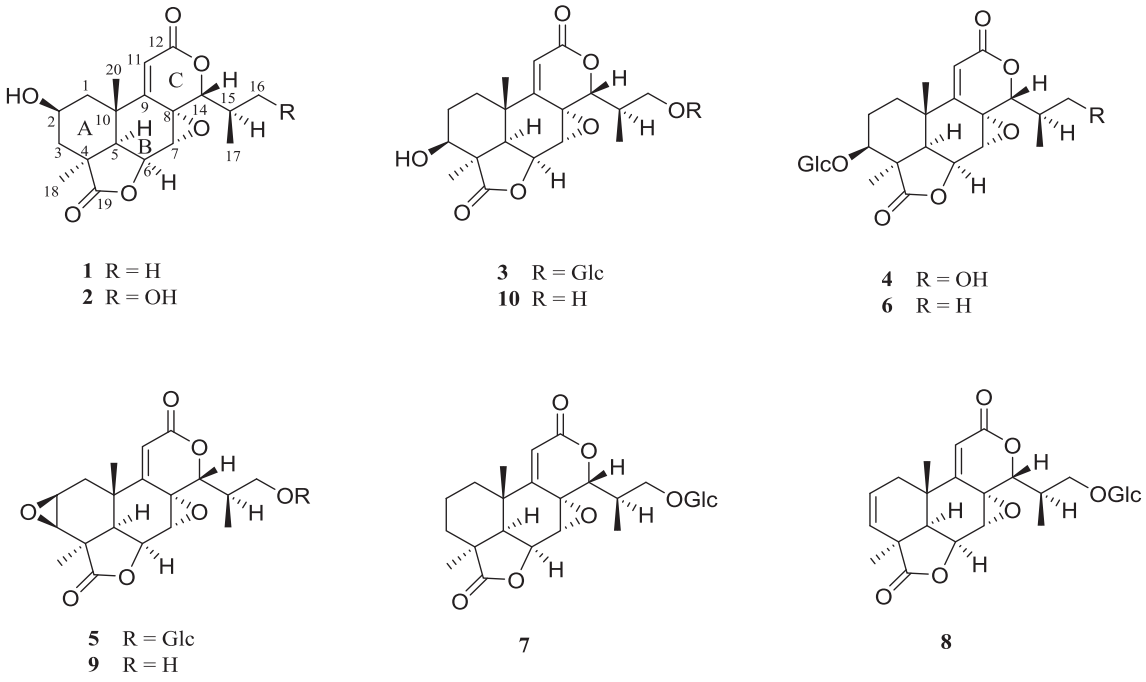

1 R = H
2 R = OH

3 R = Glc
10 R = H

4 R = OH
6 R = H

5 R = Glc
9 R = H

7

8

Chart 1. Structures of compounds **1–10**.

activity of compounds **1–3**, **5**, **9–10** were evaluated against A431, U-87 MG and A549 cell lines. The mechanism of action of compound **1** to induce cancer cells death was also studied. Compound **1** exerts its anti-proliferative activity by either arresting the cell cycle and inducing rapid apoptotic cell death. In this study, we reported the isolation and structure elucidation of new compounds, and the anti-proliferative activities of the isolates on human tumor cell lines as well.

2. Experimental

2.1. General

Silica gel (200–300, 300–400 mesh) used for column chromatography (CC) and pre-coated silica gel GF_{254} plates for TLC were produced by Qingdao Marine Chemical Industrials. Macro porous resin AB-8 (Shandong Lu Kang Chemical Industries Ltd., China), MCI gel (CHP20P, 75–150 μm, Mitsubishi Chemical Industries Ltd., Japan), polyamide (Sinopharm Chemical Reagent Co. Ltd., China) and sephadex LH-20 (Phamacia Biotech AB, Sweden) were applied for CC. Analytical HPLC (SunFire RP C_{18}, 5 μm, 4.6 × 150 mm) was applied on a Waters 2695 instrument (Milford, MD, USA) coupled with a 2998 PDA, a Waters 2424 ELSD, and a Waters 3100 MS detector. Preparative HPLC was performed on a Varian PrepStar pump with an Alltech 3300 ELSD (Columbia, MD, USA) using a Waters SunFire RP C_{18}, 5 μm, 30 × 150 mm column. NMR spectra were recorded on a Bruker Avance III (Bruker, Zurich, Switzerland) for 500 M NMR spectrometer. The chemical shift (δ) values were showed in ppm with TMS as internal standard, and coupling constants (J) were in Hz. HRESIMS were recorded on an Agilent G6520 Q-TOF mass detector and a Waters Xevo Q-Tof mass detector (Santa Clara, CA, USA). IR data were obtained using a Nicolet Magna FTIR-750 spectrophotometer (Waltham, MA, USA). Melting point was measured on a Melting-Point-Measuring Instrument (Beijing Tektronix Instrument Co., Ltd., China). Optical rotations were given by a Rudolph Autopol VI Automatic polarimeter (Hackettstown, NJ, USA). All of solvents used for CC and HPLC were analytical grade (Shanghai Chemical Reagents Co. Ltd., Shanghai, China) and gradient grade (Merck KGaA, Darmstadt, Germany), respectively.

2.2. Plant material

The twigs of *P. nagi* were collected from Ledong County, Hainan Province, China, and identified by associate Professor Chang-Qiang Ke from Shanghai Institute of Materia Medica. A voucher specimen (No. 20140611) was deposited at the herbarium of Shanghai Institute of Materia Medica, Chinese Academy of Sciences.

2.3. Extraction and isolation

Dried twigs of *P. nagi* (30 Kg) was powdered and percolated with 95% EtOH (3 × 35 L) at room temperature (72 h each). The concentrated residue (1.1 kg) was suspended in water and then partitioned successively with petroleum ether and EtOAc. The water-soluble fraction (about 600 g residue suspended in 5 L water) was subjected to column chromatography (CC) over AB-8 resin (6 L). AB-8 resin is a broad-spectrum adsorption resin with weak polarity, and is widely used in purification of natural products from crude extracts. The AB-8 column was eluted with water (20 L) and then a mixture solvent of EtOH/H_2O (40:60, v/v, 20 L; 70:30, v/v, 20 L) to produce three fractions (Fr.2A-2C). Fr·2B was chromatographed on a polyamide gel column eluted with EtOH/H_2O (10:90 to 40:60, v/v) to give three fractions (Fr·2B1–2B3). Fr·2B1 was subjected to CC over MCI gel, eluted with EtOH/H_2O (0:100 to 45:55, v/v), to yield eight fractions (Fr·2B1A-2B1H). Fractions of 2B1C and 2B1D were combined and then subjected to CC over silica gel (200–300 mesh) eluted with a dichloromethane (DCM)-MeOH solvent system (20:1 to 3:1, v/v) to yield nine sub-fractions (2B1C1–2B1C9). Sub-fraction 2B1C7 was subjected to CC over silica gel (300–400 mesh) eluted with DCM-MeOH (15:1 to 5:1, v/v) to afford compound **3** (12 mg), and a new fraction (Fr·2B1C7A), which was purified by semi-preparative HPLC (MeCN-H_2O, 5:95 to 30:70, v/v, 3 mL/min, 0–40 min) to offer compound **5** (5 mg). Fr·2B1C8 was separated on a silica gel column (300–400 mesh) eluted with DCM-MeOH (10:1 to 5:1, v/v) to yield three fraction (Fr·2B1C8A-2B1C8C). Fr·2B1C8B and 2B1C8C were purified by semi-preparative HPLC (MeCN-H_2O, 5:95 to 28:72, v/v, 3 mL/min, 0–40 min), respectively, to afford compounds **4** (3 mg), **6** (2 mg), **7** (3 mg), and **8** (3 mg).

The EtOAc-soluble was subjected to CC over a MCI gel eluted with EtOH/H_2O (20:80 to 95:5, v/v), yielding five fractions (Fr.1A-1E). Fr·1B

Table 1
^{1}H NMR data for compounds **1–4** (500 MHz, δ in ppm, J in Hz).

No.	1[a]	2[a]	3[b]	4[b]
1	1.84 (dd, 13.5, 7.5) 2.47 (dd, 13.5, 8.7)	1.82 (dd, 13.5, 7.4) 2.47 (dd, 13.5, 8.7)	1.59 (m) 1.84 (dt, 12.7, 3.6)	1.64 (dt, 12.4, 4.6) 1.85 (m)
2	4.24 (m)	4.25 (m)	1.79 (ddd, 13.8, 11.5, 4.3) 2.03 (ddd, 13.8, 6.6, 3.6)	1.93 (m) 2.27 (m)
3	2.19 (dd, 13.7, 4.8) 2.52 (t, 13.7)	2.18 (dd, 13.7, 4.9) 2.49 (m)	3.67 (m)	3.80 (dd, 10.3, 5.8)
5	1.99 (d, 5.0)	1.98 (d, 5.0)	1.94 (d, 4.1)	2.00 (d, 4.1)
6	5.18 (dd, 5.0, 1.5)	5.17 (dd, 5.0, 1.5)	5.07 (dd, 4.1, 1.5)	5.11 (dd, 4.1, 1.5)
7	4.28 (d, 1.5)	4.40 (d, 1.5)	4.29 (d, 1.5)	4.19 (d, 1.4)
11	6.35 (s)	6.32 (s)	6.00 (s)	6.02 (s)
14	4.62 (d, 3.3)	4.89 (d, 5.3)	4.82 (d, 4.5)	4.75 (d, 4.8)
15	1.98 (m)	2.30 (m)	2.21 (dt, 7.8, 4.4)	1.96 (m)
16	1.05 (d, 6.7)	4.09 (dd, 10.6, 7.2) 4.33 (dd, 10.6, 3.8)	3.63 (dd, 10.2, 7.9) 4.22 (dd, 10.2, 3.5)	3.57 (dd, 10.9, 7.4) 3.91 (dd, 10.9, 3.6)
17	1.20 (d, 6.7)	1.36 (d, 6.8)	1.22 (d, 6.8)	1.18 (d, 6.8)
18	1.34 (s)	1.34 (s)	1.49 (s)	1.54 (s)
20	1.31 (s)	1.34 (s)	1.24 (s)	1.27 (s)
1′			4.30 (d, 7.8)	4.40 (d, 7.7)
2′			3.18 (dd, 9.2, 7.8)	3.30 (m)
3′			3.36 (t, 8.7)	3.38 (m)
4′			3.28 (m)	3.31 (m)
5′			3.29 (m)	3.31 (m)
6′			3.69 (dd, 11.9, 5.0) 3.91 (dd, 11.9, 2.0)	3.69 (dd, 11.9, 5.2) 3.87 (dd, 11.9, 1.8)

[a] In pyridine-d_5.
[b] In methanol-d_4.

was subjected to CC over silica gel (200–300 mesh) eluted with a DCM-MeOH solvent system (80:1 to 10:1, v/v) to yield 10 sub-fractions (1B1–1B10). Fr·1B5 was purified by CC over Sephadex LH-20 gel eluted with $CHCl_3$/MeOH (1:1, v/v) to yield three fractions (1B5A–1B5C). Fr·1B5B was subjected to CC over silica gel (300–400 mesh) eluted with DCM-MeOH (40:1 to 20:1, v/v) to yield fractions 1B5B1-1B5B4. Compounds **2** (30 mg) and **10** (10 mg) were obtained from Fr·1B5B3 by preparative HPLC (MeCN/H_2O, 10:90 to 50:50, v/v, 25 mL/min, 0–110 min). Fr·1B6 was subjected to CC over Sephadex LH-20 gel eluted with $CHCl_3$/MeOH (1:1) to give four fractions (1B6A-1B6D). Fr·1B6B was purified by CC over silica gel (300–400 mesh) eluted with DCM-MeOH (40:1 to 20:1, v/v) to yield four fractions (1B6B2-1B6B5), and a pure compound **9** (60 mg). Compound **1** (9 mg) was separated from Fr·1B6B3 by semi-preparative HPLC (MeCN/H_2O, 10:90 to 45:55, v/v, 3 mL/min, 40 min).

2.3.1. 3-Deoxy-2β-hydroxynagilactone E (1)

White amorphous powder; MP, 274–276 °C; $[\alpha]_D^{20}$ + 57 (*c* 0.1, MeOH); IR ν_{max} (KBr) 3424, 2971, 1771, 1718, 1695, 1385, 1265, 1169, 1055, 1030 cm^{-1}; ^{1}H and ^{13}C NMR data see Tables 1 and 2; HRESIMS *m/z* 349.1645 $[M + H]^+$ (calcd for $C_{19}H_{25}O_6$, 349.1646).

2.3.2. 3-Deoxy-2β,16-dihydroxynagilactone E (2)

White amorphous powder; MP, 243–245 °C; $[\alpha]_D^{20}$ + 90 (*c* 0.1, MeOH); IR ν_{max} (KBr) 3445, 2924, 1758, 1706, 1541, 1459, 1069 cm^{-1}; ^{1}H and ^{13}C NMR data see Tables 1 and 2; HRESIMS *m/z* 365.1594 $[M + H]^+$ (calcd for $C_{19}H_{25}O_7$, 365.1595).

2.3.3. 16-O-β-D-Glucopyranosylnagilactone E (3)

White amorphous powder; MP, 180–183 °C; $[\alpha]_D^{20}$ + 4 (*c* 0.1, MeOH); IR ν_{max} (KBr) 3403, 2939, 1780, 1697, 1274, 1066, 1026, 1015 cm^{-1}; ^{1}H and ^{13}C NMR data see Tables 1 and 2; HRESIMS *m/z* 527.2114 $[M + H]^+$ (calcd for $C_{25}H_{35}O_{12}$, 527.2123).

2.3.4. 3-O-β-D-Glucopyranosyl-16-hydroxynagilactone G (4)

White amorphous powder; $[\alpha]_D^{20}$ − 21 (*c* 0.1, MeOH); IR ν_{max} (KBr) 3406, 2926, 1755, 1722, 1598, 1404, 1255, 1094, 1043, 1022 cm^{-1}; ^{1}H and ^{13}C NMR data see Tables 1 and 2; HRESIMS *m/z* 527.2115 $[M + H]^+$ (calcd for $C_{25}H_{35}O_{12}$, 527.2123).

2.3.5. 2,3-β-Epoxy-16-O-β-D-glucopyranosylnagilactone G (5)

White amorphous powder; $[\alpha]_D^{20}$ + 24 (*c* 0.1, MeOH); IR ν_{max} (KBr) 3436 (strong), 2930, 1769, 1702, 1598, 1420, 1383, 1124, 1089, 1032 cm^{-1}; ^{1}H and ^{13}C NMR data see Tables 2 and 3; HRESIMS *m/z* 525.1959 $[M + H]^+$ (calcd for $C_{25}H_{33}O_{12}$, 525.1967).

2.3.6. 3-O-β-D-Glucopyranosylnagilactone G (6)

White amorphous powder; $[\alpha]_D^{20}$ − 7 (*c* 0.1, MeOH); IR ν_{max} (KBr) 3436, 2928, 1761, 1714, 1383, 1224, 1081, 1040 cm^{-1}; ^{1}H and ^{13}C NMR data see Tables 2 and 3; HRESIMS *m/z* 533.1993 $[M + Na]^+$ (calcd for $C_{25}H_{34}O_{11}Na$, 533.1993).

2.3.7. 16-O-β-D-Glucopyranosylnagilactone G (7)

White amorphous powder; $[\alpha]_D^{20}$ + 8 (*c* 0.1, MeOH); IR ν_{max} (KBr) 3426, 2922, 1765, 1716, 1698, 1255, 1079, 1045 cm^{-1}; ^{1}H and ^{13}C NMR data see Tables 2 and 3; HRESIMS *m/z* 533.1988 $[M + Na]^+$ (calcd for $C_{25}H_{34}O_{11}Na$, 533.1993).

2.3.8. 2,3-Dehydro-16-O-β-D-glucopyranosylnagilactone G (8)

White amorphous powder; $[\alpha]_D^{20}$ − 19 (*c* 0.1, MeOH); IR ν_{max} (KBr) 3414, 2932, 1775, 1706, 1384, 1257, 1169, 1083, 1030, 945 cm^{-1}; ^{1}H and ^{13}C NMR data see Tables 2 and 3; HRESIMS *m/z* 531.1833 $[M + Na]^+$ (calcd for $C_{25}H_{32}O_{11}Na$, 531.1837).

2.4. Glycosides hydrolyzed and carbohydrate identified

Compound **3** (2 mg) in MeOH (5 mL) was added 2 N HCl (5 mL) and heated at 80 °C for 2 h. The resulting reaction solution was extracted twice with CH_2Cl_2 (6 mL), and the aqueous layers containing sugars was concentrated. The concentrate aforementioned was heated with *L*-cysteine methyl ester hydrochloride in pyridine for 1 h at 60 °C, and then *O*-tolylisothiocyanate was added to the reaction mixture and further reacted at 60 °C for another 1 h. Sugar standards (D/L-glucose) purchased were derivatized in the same method. The reaction mixtures were analyzed by HPLC, eluted with CH_3CN-H_2O (20:80 to 35:65, 1.0 mL/min, 25 min) containing 0.1% formic acid, and detected with a UV detector (210–400 nm) at 30 °C. The retention time of D-glucose standard derivative was 13.17 min, which different from that of L-glucose standard, 12.35 min. Compared the retention time of sugar derivative of these compounds with those of sugar standards, D-glucose was determined from compound **3**.

2.5. X-ray crystallographic analyses

Colorless crystals of compounds **1–3** were obtained by recrystallization in a mixture solvent of MeOH/H_2O at 4 °C. Data collections were performed with a Bruker SMART-APEX II ULTRA CCD area detector with graphite monochromated Cu-Kα radiation (λ = 1.54178 Å). The structures were refined with full-matrix least-squares calculations on *F*2 using SHELXL-2014 (Sheldrick, 2014). Full details of the data collection and refinement and tables of atomic coordinates, bond lengths and angles, and torsion angles have been deposited with the Cambridge Crystallographic Data Center.

3-Deoxy-2β-hydroxynagilactone E (**1**). $C_{19}H_{24}O_6$, M = 348.38, monoclinic, space group $P2_12_12_1$; a = 7.7966 (2) Å, b = 12.1822 (3) Å, c = 17.6340 (4) Å, α = 90°, β = 90°, γ = 90°; V = 1674.87 (7) $Å^3$,

Table 2
^{13}C NMR Data (δ in ppm) for Compounds **1–8** (125 MHz).

No.	1[a]	2[a]	3[b]	4[b]	5[b]	6[b]	7[b]	8[b]
1	41.1, t	41.0, t	30.1, t	29.8, t	31.3, t	29.8, t	30.5, t	33.4, t
2	64.2, d	64.2, d	29.0, t	28.0, t	53.0, d	28.0, t	18.6, t	127.4, d
3	39.0, t	39.0, t	73.9, d	83.7, d	53.6, d	83.8, d	29.5, t	129.1, d
4	42.8, s	42.8, s	46.2, s	47.4, s	44.2, s	47.4, s	43.2, s	45.4, s
5	42.7, d	42.7, d	46.4, d	46.3, d	44.2, d	46.3, d	44.8, d	44.3, d
6	73.5, d	73.5, d	73.8, d	73.7, d	74.5, d	73.8, d	74.1, d	73.5, d
7	54.8, d	55.4, d	55.5, d	55.4, d	55.3, d	54.9, d	55.4, d	55.3, d
8	58.5, s	58.3, s	59.5, s	59.2, s	59.0, s	59.5, s	59.2, s	58.7, s
9	159.8, s	160.0, s	161.1, s	161.2, s	160.7, s	161.7, s	161.7, s	160.5, s
10	37.5, s	37.5, s	37.7, s	37.3, s	36.7, s	37.3, s	37.3, s	36.7, s
11	118.9, d	118.6, d	117.1, d	117.3, d	117.3, d	117.4, d	117.3, d	117.8, d
12	164.4, s	164.3, s	165.8, s	165.7, s	165.7, s	166.2, s	165.9, s	165.8, s
14	83.2, d	82.7, d	83.3, d	83.6, d	83.3, d	84.4, d	83.3, d	83.2, d
15	27.4, d	35.3, d	33.8, d	35.0, d	33.8, d	27.8, d	33.8, d	33.8, d
16	21.8, q	63.0, t	72.3, t	63.5, t	72.2, t	21.6, q	72.3, t	72.4, t
17	17.0, q	16.6, q	16.3, q	16.1, q	16.3, q	16.6, q	16.3, q	16.3, q
18	23.4, q	23.4, q	22.0, q	21.9, q	21.4, q	21.9, q	24.4, q	22.9, q
19	181.8, s	181.8, s	179.5, s	179.2, s	179.0, s	179.3, s	182.6, s	180.1, s
20	29.3, q	29.0, q	24.2, q	24.6, q	26.2, q	24.8, q	25.1, q	23.5, q
1′			105.5, d	107.6, d	105.5, d	107.6, d	105.5, d	105.6, d
2′			75.2, d	75.3, d	75.2, d	75.3, d	75.2, d	75.3, d
3′			78.0, d	77.8, d	78.0, d	77.8, d	78.0, d	78.1, d
4′			71.7, d	71.6, d	71.7, d	71.6, d	71.7, d	71.7, d
5′			78.0, d	78.1, d	78.0, d	78.1, d	78.0, d	78.1, d
6′			62.8, t	62.8, t	62.8, t	62.8, t	62.8, t	62.8, t

[a] In pyridine-d_5.
[b] In methanol-d_4.

Table 3
^{1}H NMR data for compounds **5–8** (500 MHz, δ in ppm, J in Hz, in methanol-d_4).

No.	5	6	7	8
1	1.94 (brd, 14.7)	1.62 (dt, 12.3, 4.6)	1.52 (m)	2.22 (m)
	2.35 (dd, 14.8, 2.2)	1.84 (m)	1.72 (m)	2.22 (m)
2	3.46 (m)	1.94 (m)	1.68 (m)	5.94 (ddd, 9.8, 4.8, 3.2)
		2.01 (m)	1.68 (m)	
3	3.19 (d, 2.8)	3.80 (dd, 10.2, 5.8)	1.47 (m)	5.83 (dd, 9.9, 1.9)
			2.12 (m)	
5	1.86 (d, 4.6)	1.99 (d, 4.2)	1.90 (d, 4.4)	2.14 (d, 4.8)
6	5.09 (dd, 4.6, 1.4)	5.09 (dd, 4.2, 1.5)	5.04 (dd, 4.4, 1.4)	5.12 (dd, 4.8, 1.4)
7	4.29 (d, 1.4)	4.15 (d, 1.5)	4.25 (d, 1.4)	4.31 (d, 1.4)
11	6.02 (s)	6.02 (s)	5.96 (s)	6.04 (s)
14	4.79 (d, 4.6)	4.65 (d, 3.2)	4.78 (d, 4.5)	4.85 (overlapped)
15	2.20 (m)	2.26 (m)	2.18 (m)	2.22 (m)
16	3.63 (dd, 10.1, 7.9)	1.10 (d, 6.8)	3.60 (dd, 10.2, 7.9)	3.64 (dd, 10.2, 7.9)
	4.20 (dd, 10.2, 3.5)		4.20 (dd, 10.2, 3.5)	4.23 (dd, 10.2, 3.4)
17	1.22 (d, 6.8)	1.09 (d, 6.8)	1.18 (d, 6.8)	1.24 (d, 6.8)
18	1.51 (s)	1.54 (s)	1.26 (s)	1.37 (s)
20	1.28 (s)	1.26 (s)	1.12 (s)	1.19 (s)
1′	4.30 (d, 7.6)	4.40 (d. 7.7)	4.26 (d, 7.8)	4.30 (d, 7.8)
2′	3.18 (dd, 9.2, 7.8)	3.30 (m)	3.15 (dd, 9.2, 7.8)	3.19 (dd, 9.2, 7.8)
3′	3.36 (t, 8.8)	3.38 (m)	3.33 (t, 8.8)	3.36 (t, 8.7)
4′	3.28 (m)	3.31 (m)	3.25 (m)	3.29 (m)
5′	3.29 (m)	3.30 (m)	3.27 (m)	3.29 (m)
6′	3.68 (dd, 11.9, 5.5)	3.68 (dd, 11.9, 5.0)	3.66 (dd, 11.9, 5.4)	3.69 (dd, 11.9, 5.4)
	3.91 (dd, 11.8, 2.0)	3.89 (dd, 11.8, 1.7)	3.88 (dd, 11.9, 2.0)	3.90 (dd, 11.9, 2.0)

Z = 4, T = 173 K, D_{calc} = 1.382 Mg/m^3; 13,556 reflections measured, 3068 independent reflections (R_{int} = 0.037). The final R_1 values were 0.0302 ($I > 2\delta$ (I)). The final $wR(F_2)$ values were 0.0790 ($I > 2\delta$ (I)). Flack parameter = 0.02 (7). The X-ray diffraction material has also been deposited in the Cambridge Crystallographic Data Center (CCDC 1562849).

3-Deoxy-2β,16-dihydroxynagilactone E (**2**). $C_{19}H_{24}O_7$·O, M = 380.38, monoclinic, space group $P2_12_12_1$; a = 6.3077 (2) Å, b = 12.6888 (5) Å, c = 22.6305 (8) Å, α = 90°, β = 90°, γ = 90°; V = 1811.28 (11) Å^3, Z = 4, T = 293 K, D_{calc} = 1.395 Mg/m^3; 16,719 reflections measured, 3318 independent reflections (R_{int} = 0.052). The final R_1 values were 0.0391 ($I > 2\delta$ (I)). The final $wR(F_2)$ values were 0.1054 ($I > 2\delta$ (I)). Flack parameter = 0.0 (2). The X-ray diffraction material has also been deposited in the Cambridge Crystallographic Data Center (CCDC 1562850).

16-*O*-β-D-Glucopyranosylnagilactone E (**3**). $C_{25}H_{34}O_{12}$.3.5H_2O.0.5O, M = 598.58, monoclinic, space group $P2_12_12_1$; a = 7.8034 (2) Å, b = 9.5475 (3) Å, c = 39.8398 (11) Å, α = 90°, β = 90°, γ = 90°; V = 2968.18 (15) Å^3, Z = 4, T = 293 K, D_{calc} = 1.258 Mg/m^3; 27,457 reflections measured, 5424 independent reflections (R_{int} = 0.0485). The final R_1 values were 0.0771 ($I > 2\delta$ (I)). The final $wR(F_2)$ values were 0.2176 ($I > 2\delta$ (I)). Flack parameter = 0.1 (3). The X-ray diffraction material has also been deposited in the Cambridge Crystallographic Data Center (CCDC 1562848).

2.6. Cytotoxic bioactivity

2.6.1. Cell culture and reagents

A431, U-87 MG and A549 cells were obtained from ATCC (American Type Culture Collection Rockville, MD, USA). A431 and U-87 MG were maintained in Dulbecco's modified Eagle's medium (DMEM) while A549 cells were cultured with RPMI 1640 medium supplemented with heat-inactivated 10% fetal bovine serum (FBS), glutamine and antibiotics (penicillin and streptomycin) at 37 °C in a humidified 5% CO_2 atmosphere. Combretastatin A4 (CA-4) served as a positive control (SelleckChem S7204). Paclitaxel (Taxol) was purchased from SelleckChem (S1150).

2.6.2. Cell viability assay

Cell proliferation was determined using the Sulforhodamine B assay for cytotoxicity screening (Sigma-Aldrich). Briefly, cells were seeded in 96-well plates (4 × 10^3 cells/well) overnight and exposed to various concentrations of compound **1** or CA-4 for 72 h, subsequently were

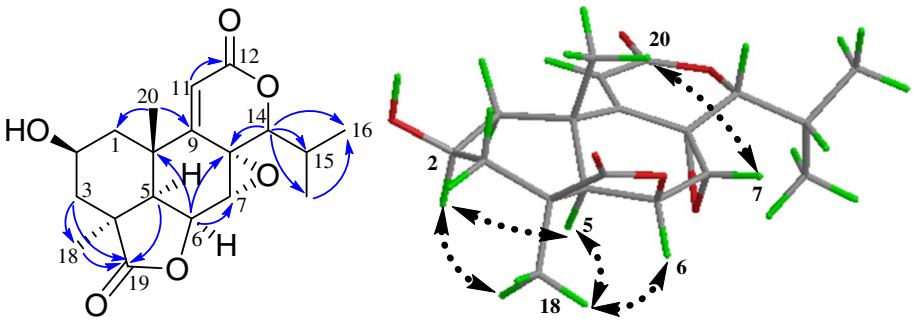

Fig. 1. Key HMBC (→) and NOESY (←---→) correlations of compound **1**.

fixed in TCA solution at 4 °C for 1 h. Cell proliferation was evaluated by protein labelling with 0.4% Sulforhodamine B solution and optical density was measured using a multi-well spectrophotometer (VERSA max™, Molecular Devices, Sunnyvale, CA, USA) at 560 nm. The inhibitory rates (%) of compounds were calculated with the following formula: $[1 - (A_{560\ treated} / A_{560\ control})] \times 100\%$. The IC_{50} was determined from a curve derived from a log (inhibitor) *vs.* response - Variable slope (four parameters) equation and fit in GraphPad Prism 7.

2.6.3. Western blot analysis

A431 cells were incubated for 24 h or 48 h with or without compound **1** to chemically induce cell cycle and apoptosis. The detailed procedure of whole cell extracts were prepared as previously described [26]. Samples were analyzed by SDS-PAGE and proteins were detected by immunoblot and Pico assay. Proteins were detected by the following antibodies: anti-*β*-actin (66009-1-Ig), anti-rabbit (515-005-003) and anti-mouse (715-005-140) IgG were from proteintech. Antibodies against PARP1 (#9532), Caspase-3 (#9962), cleaved-caspase-3 (#9961), p-Rb (#2181), Rb (#9309), CyclinD1 (#2922) and CDK6 (#3136) were obtained from Cell Signaling Technology (Danvers, USA). Anti-mouse monoclonal antibody p21 (sc-817) were provided by Santa Cruz Biotechnology.

2.6.4. Flow cytometry

Annexin V-Fluorescein isothiocyanate (FITC) and Propidium Iodide (PI) double staining were utilized for detecting apoptosis cells. A431, U-87 MG and A549 cells were treated with 0.1% DMSO (negative control), Paclitaxel (Positive control) and compound **1** at the indicated concentrations in 37%, 5% CO_2 incubation. Cell cycle arrest was determined by the incorporation of PI (Beyotime Biotechnology) into permeabilized cells *via* 70% ethanol overnight after 24 h. Cells undergoing apoptosis within 48 h were identified using an Annexin-V-FITC Apoptosis Detection kit (Vazyme Biotech.) according to the manufacturer's instructions.

2.6.5. Statistics

Most results are presented as the mean ± SD. Standard deviation analyses were systematically carried out for three or more sample conditions and mean values were compared with the Student's *t*-test using the Prism software (GraphPad Software, La Jolla, USA). Significance threshold was fixed at $*p < 0.05$, $**p < 0.01$, $***p < 0.001$.

3. Results and discussion

3.1. Structural elucidation

Chromatography of the EtOAc-soluble and water-soluble fractions of the 95% ethanol extract from the twigs of *P. nagi* over macro porous resin AB-8, silica gel, MCI gel, Sephadex LH-20, and preparative HPLC with different solvent systems afforded 10 type B nagilactones (**1** − **10**).

Compound **1** was obtained as colorless crystals from a mixture solution of MeOH/H_2O. Its molecular formula was determined to be $C_{19}H_{24}O_6$ by the protonated molecular ion at *m/z* 349.1645 ($[M + H]^+$, calcd for $C_{19}H_{25}O_6$, 349.1646) in HRESIMS, corresponding to eight degrees of unsaturation. IR absorption bands at 3424, 1771, and 1695 cm^{-1} indicated the presence of hydroxy, γ-lactone and *δ*-lactone carbonyl groups, respectively. The ^1H NMR spectrum of compound **1** (Table 1) displayed signals of seven methines, including an olefinic proton (δ_H 6.35, s, H-11) and four oxygenated methines (δ_H 5.18, dd, J = 5.0, 1.5 Hz, H-6; 4.28, d, J = 1.5 Hz, H-7; 4.62, d, J = 3.3 Hz, H-14; 4.24, m, H-2), two methylenes, two singlet methyls (δ_H 1.34, H_3–18; 1.31, H_3–20), and two doublet methyls (δ_H 1.20, J = 6.7 Hz, H_3-16; 1.05, J = 6.7 Hz, H_3-17). A total of 19 carbon resonances were present in the ^{13}C NMR spectrum (Table 2) ascribed to four methyls, two methylenes, seven methines [one olefinic (δ_C 118.9) and four oxygenated (δ_C 83.2, 73.6, 64.2 and 54.8)], and six quaternary carbons [two ester carbonyl (δ_C 181.8, 164.4), one olefinic (δ_C 159.8), and one oxygenated (δ_C 58.5)]. The oxygenated methines (δ_C 83.2, C-14; 54.8, C-7) and the quaternary carbons (δ_C 159.8, C-12; 118.9, C-11; 58.5, C-8) suggested the existence of a characteristic 7*α*,8*α*-epoxy-9(11)-enolide moiety [11]. Furthermore, ^1H and ^{13}C NMR data of **1** were quite similar to those of 3-deoxy-2*α*-hydroxynagilactone E [27–28]. Detailed analysis of the HSQC and HMBC spectra (Fig. 1) resulted in the construction of compound **1**, which shared the same planar structure with 3-deoxy-2*α*-hydroxynagilactone E. The relative configuration of **1** was deduced from the NOESY experiment (Fig. 1). The correlations of H-2/H_3-18, H-2/H-5, H-6/H_3-18 and H-5/H_3-18 implied that H-2, H-5, H-6 and H_3-18 were co-facial, and thus OH-2 was on the other face. The *α*-orientation of 7,8-epoxy was assigned based on the correlations from H_3-20 to H-7. The full structure including the absolute configuration of compound **1** were confirmed by the X-ray single crystal diffraction analysis (Fig. 2). Therefore, compound **1** was structurally established, and named 3-deoxy-2*β*-hydroxynagilactone E.

Compound **2** was isolated as a white amorphous powder. A pronated molecular ion at *m/z* 365.1594 ($[M + H]^+$, calcd for $C_{19}H_{25}O_7$,

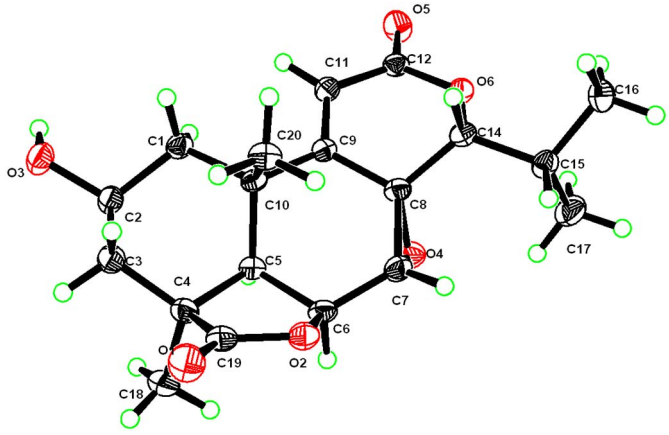

Fig. 2. Perspective ORTEP drawing for compound **1**.

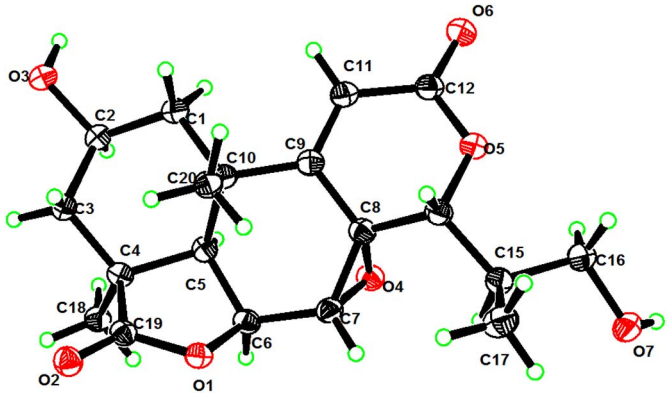

Fig. 3. Perspective ORTEP drawing for compound **2**.

365.1595) in HRESIMS was indicative of a molecular formula $C_{19}H_{24}O_7$ with eight indices of hydrogen deficiency. The IR spectrum showed the bands at 3445, 1758, and 1706 cm^{-1} due to the presence of hydroxy, γ-lactone, and δ-lactone carbonyl groups, respectively. The NMR data (Tables 1 and 2) were closely related to those of **1** except that an oxymethylene (δ_H 4.33, dd, J = 10.6, 3.8 Hz; 4.09, dd, J = 10.6, 7.2 Hz) rather than a methyl were present in the structure of **2**. The presence of the oxymethylene group was permitted locating at C-16 by the HMBC correlations from H-14 (δ_H 4.89, d, J = 5.3 Hz) to C-16 (δ_C 63.0, t), and from H_2-16 to C-17 (δ_C 16.6). The relative configuration of **2** was assigned on the basis of extensive analysis of the NOESY spectrum. The correlations of H-2/H-5, and H-7/H_3-20 suggested the orientation of OH-2 and 7,8-epoxy as *β* and *α*, respectively, the same with that of compound **1**. The X-ray single crystal diffraction analysis further confirmed the full structure of **2** (Fig. 3). Therefore, compound **2** was defined, and named 3-deoxy-2*β*,16-dihydroxysnagilactone E.

Compound **3** was obtained as a white amorphous powder. Its molecular formula was deduced as $C_{25}H_{34}O_{12}$ by a HRESIMS pronated molecular ion at *m/z* 527.2114 ($[M + H]^+$, calcd for $C_{25}H_{35}O_{12}$, 527.2123), corresponding to nine degrees of unsaturation. The IR spectrum exhibited absorption bands at 3403 cm^{-1} for hydroxy, 1780 cm^{-1} for γ-lactone, and 1698 cm^{-1} for δ-lactone carbonyl groups, respectively. Analysis of the ^1H and ^{13}C NMR data (Tables 1 and 2) revealed that **3** was related closely to the known compound 16-hydroxynagilactone E (**10**), except for additional signals attributed to a glucose unit (δ_C 105.5, 78.0, 78.0, 75.2, 71.7, 62.8; δ_H 4.30, d, J = 7.8 Hz). The major fragment ion at *m/z* 365 $[M - 162]^+$ in the ESIMS spectrum also suggested the existence of a glucose unit. The configuration of the anomeric proton of the glucose was assigned as *β* configuration based on the coupling constant. Acid hydrolysis and derivatization reaction for the released sugar was applied to identify the D-configuration of the glucose [29–30]. The location of the sugar moiety was manifested to be at C-16 by the HMBC correlations from the anomeric proton (δ_H 4.30, d, J = 7.8 Hz) to C-16 (δ_C 72.3, t), and by the glucosylation shift of C-16 (δ_C 72.3, **3***vs* 63.0, **2**) (Fig. 4). The cross-peaks of H-3/H-5, H-3/H_3–18 in the NOESY spectrum designated a *β*-orientation for OH-3, and the cross-peaks of H-7/H_3-20 suggested the orientation of 7,8-epoxy to be *α* (Fig. 4). Furthermore, X-ray single crystal diffraction analysis confirmed the absolute configuration (Fig. 5). Accordingly, **3** was structurally established, and named 16-*O*-*β*-D-glucopyranosylnagilactone E.

Compound **4** was obtained as a white amorphous powder. The HRESIMS indicated a molecular formula of $C_{25}H_{34}O_{12}$ from the pronated molecular ion at *m/z* 527.2115 ($[M + H]^+$, calcd for $C_{25}H_{35}O_{12}$, 527.2123). Its ESIMS spectrum showed a typical fragment ion at *m/z* 365 $[M - 162]^+$, indicating the presence of a glucose unit. The NMR data (Tables 1 and 2) of **4** quite resembled those of **3** except for the

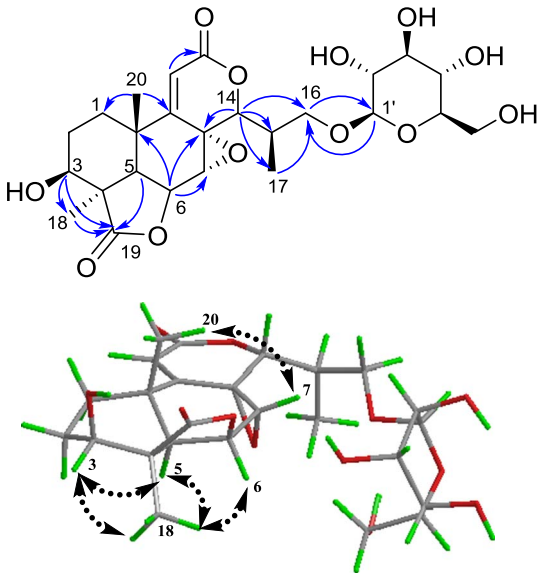

Fig. 4. Key HMBC (→) and NOESY (←---→) correlations of compound **3**.

chemical shift differences observed for C-3 (δ_C 83.7, **4***vs* 73.9, **3**) and C-16 (δ_C 63.5, **4***vs* 72.3, **3**). Detailed analysis of the HMBC data revealed that the sugar moiety was attached to C-3 rather than C-16, which could be clearly inferred from the HMBC correlations from H-3 (δ_H 3.80, dd, J = 10.3, 5.8 Hz) to the anomeric carbon (δ_C 107.6). Moreover, NOESY correlations of H-3/H-5, H-3/H_3-18, and H-6/H_3-18 demonstrated that H-3 was *α*-oriented, and those of H-7/H_3-20 suggested an *α*-orientation of the 7,8-epoxy. Thus, the structure of compound **4** was determined, and named 3-*O*-*β*-D-glucopyranosyl-16-hydroxylnagilactone G.

Compound **5**, a white amorphous powder, gave a molecular formula of $C_{25}H_{32}O_{12}$ ($[M + H]^+$, calcd for $C_{25}H_{33}O_{12}$, 525.1959) with 10 degrees of unsaturation, based on its HRESIMS. Its ESIMS spectrum indicated the existence of a glucose unit deduced from the presence of a fragment ion at *m/z* 363 $[M - 162]^+$. The NMR data of **5** (Tables 2 and 3) and **3** were found to be quite comparable except for the obvious chemical shift differences observed for C-2 (δ_C 53.0, **5***vs* 29.0, **3**) and C-3 (δ_C 53.6, **5***vs* 73.9, **3**). Compared with **3**, compound **5** had one more degree of unsaturation and two protons less in the molecular formula, suggesting the existence of an epoxy located at C-2/C-3. Such elucidation was further supported by correlations from H-2 (δ_H 3.46, m) to C-10 (δ_C 36.7), and from H_3-18 (δ_H 1.51, s) to C-3 (δ_C 53.6) in the HMBC spectrum. The *β*-orientation of 2,3-epoxy was assigned based on the correlations of H-2/H-5, H-3/H-5, H-2/H_3-18, and H-3/H_3-18 in the NOESY spectrum. Therefore, the structure of compound **5** was established, and named 2,3-*β*-epoxy-16-O-*β*-D-glucopyranosylnagilactone G.

The molecular formula of compound **6** was deduced as $C_{25}H_{34}O_{11}$ by HRESIMS (533.1993 $[M + Na]^+$, calcd for $C_{25}H_{34}NaO_{11}$). Its ESIMS spectrum exhibited a fragment ion at 349 $[M - 162]^+$, indicative of the presence of a sugar unit. A detailed comparison of the NMR spectroscopic data (Tables 2 and 3) of **6** with those of **4** revealed the presence of an additional methyl (δ_C 21.6) and the absence of an oxymethylene (δ_C 63.5) in **6**. Such structural changes occurring at C-16 was supported by tcorrelations from H-14 (δ_H 4.65, d, J = 3.2 Hz) and H_3-17 (δ_H 1.09, d, J = 6.8 Hz) to C-16 (δ_C 21.6) in the HMBC spectrum. Cross-peaks of H-3/H-5, H-3/H_3-18, and H-6/H_3-18 in the ROESY spectrum assigned an *α*-orientation of H-3, and those of H-7/H_3-20 suggested also an *α*-orientation of the 7,8-epoxy. Thus, the structure of compound **6** was proposed, and named 3-*O*-*β*-D-glucopyranosylnagilactone G.

Compound **7** shared the same molecular formula $C_{25}H_{34}O_{11}$ with **6**, as deduced from its HRESIMS spectrum. The typical fragment ion at

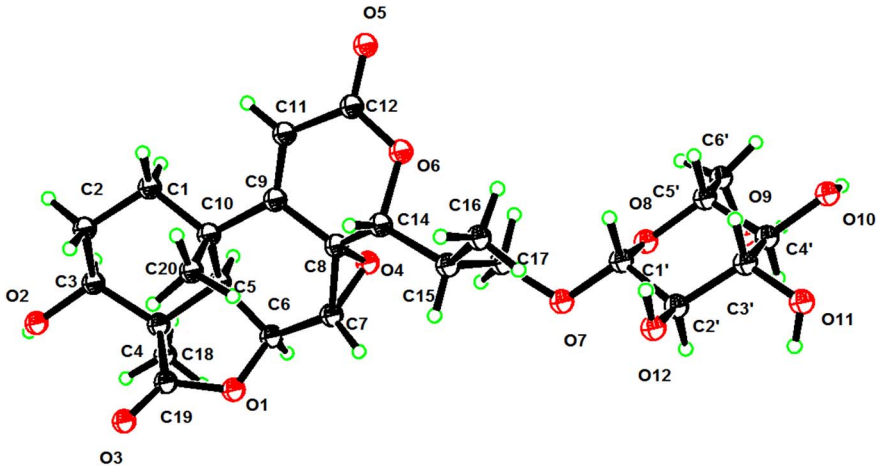

Fig. 5. Perspective ORTEP drawing for compound **3**.

349 $[M - 162]^+$ was also observed in the ESIMS, suggesting the presence of a sugar moiety. When comparing NMR data of **7** with those of **6** (Tables 2 and 3), the significant upfield shift of C-3 (δ_C 29.5, **7***vs* 83.8, **6**) and downfield shift of C-16 (δ_C 72.3, **7***vs* 21.6, **6**) suggested that the glucose unit could be placed at C-16 rather than at C-3 in compound **7**. The correlations from the anomeric proton (δ_H 4.26, d, J = 7.8 Hz) to C-16 (δ_C 72.3, t) in the HMBC spectrum also manifested the location of the sugar moiety. Thus, the structure of compound **7** was defined, and named 16-*O*-*β*-D-glucopyranosylnagilactone G.

Compound **8**, a white amorphous powder, exhibited a molecular formula of $C_{25}H_{32}O_{11}$ ($[M + Na]^+$, calcd for $C_{25}H_{32}NaO_{11}$, 531.1837) with 10 degrees of unsaturation, determined by HRESIMS, and the existence of a sugar moiety, inferred from a fragment ion at 347 $[M - 162]^+$ in ESIMS. The IR absorption bands at 3414, 1775, 1706, 1083, and 1031 cm^{-1} indicated the presence of hydroxy, γ-lactone, *δ*-lactone and double bond groups, respectively. Comparison of NMR data (Tables 2 and 3) of **8** with those of **7** revealed high similarities between these two compounds, excluding the signals of a double bond [H-2 (δ_H 5.94, ddd, J = 9.8, 4.8, 3.2 Hz), C-2 (δ_C 127.4); H-3 (5.83, dd, J = 9.9, 1.9 Hz), C-3 (δ_C 129.1)] in **8**. The HMBC correlations from H_3-18 to C-3, H_3-20 to C-1, and H-3 to C-5 suggested that the double bond was located at C-2 and C-3, which was further supported by the cross-peaks of H-1/H-2, and H-2/H-3 in the ^1H-^1H COSY spectrum. The *α*-orientation of 7,8-epoxy was assigned based on the correlations of H-7/H_3–20 in the NOESY spectrum. The structure of **8** was finally established, and named 2,3-dehydro-16-*O*-*β*-D-glucopyranosylnagilactone G.

In addition, the sugar moieties of compounds **4–8** were identified as D-glucose by comparing the NMR spectra with those of compound **3**.

Compounds **9** and **10** were identified as sellowin A [31] and 16-hydroxylnagilactone E [32], respectively, by comparison of the physical and spectroscopic data with those reported in literatures.

3.2. Bioactivity evaluation

3.2.1. Compound 1 dose-dependently inhibits the proliferation of cancer cells

Considering that series of nagilactones natural products had been identified as cytotoxic agents to tumor cells [33], we investigated the antiproliferative activity of compounds **1–3**, **5**, **9–10** in several types of human cancer cells including human epithelial carcinoma A431 cells, human glioblastoma U-87 MG cells, and human lung adenocarcinoma A549 cells. CA-4, a microtubule-depolymerizing agent, was used as a positive control compound [34–35]. The result revealed that aglycones of nagilactones (compounds **1**, **2**, **9** and **10**) exhibited moderate to strong cytotoxic bioactivity, while the glycosylated nagilactones (compounds **3** and **5**) were inactive (Table 4). Among the aglycones of nagilactones, compound **1** produced potent cytotoxicity against A431, A549 and U-87 MG cells with IC_{50} at 0.208 μM, 0.574 μM and 0.429 μM, respectively (Table 4). Additionally, compounds **2**, **9** and **10** exhibited moderate cytotoxicity against these human tumor cells with IC_{50} values ranging from 1.09 μM to 11.2 μM. The results indicated that aglycones of nagilactones possessed potent anti-tumor activities against different types of cancer.

Table 4
Antiproliferative activities of compounds **1–3**, **5**, **9–10** against the A431, A549 and U-87 MG cell lines.

Cpds	IC_{50} values (μM)		
	A431	A549	U-87 MG
1	0.208 ± 0.056	0.574 ± 0.038	0.429 ± 0.023
2	1.74 ± 0.21	1.41 ± 0.35	1.38 ± 0.19
3	> 50.0	> 50.0	> 50.0
5	> 50.0	> 50.0	> 50.0
9	8.39 ± 1.48	4.43 ± 1.74	11.2 ± 3.0
10	4.62 ± 0.44	1.09 ± 0.05	3.95 ± 0.45
CA-4	0.104 ± 0.002	0.006 ± 0.003	0.009 ± 0.000

3.2.2. Compound 1 induced A431 cells death by triggering apoptosis

To gain insights into the underlying mechanism for cell growth inhibition of compound **1**, we further examined the induction of apoptosis by this compound in cancer cells. Paclitaxel (Taxol), a potent cytotoxic anti-cancer agent was used as a positive control compound [36–37]. The results revealed that the treatment with compound **1** led to a dose-dependent increase in apoptosis of A431, U-87 MG and A549 cells, respectively (Fig. 6A). For example, approximately 18.3% of A431 cells underwent apoptosis following compound **1** treatment at 1 μM, and around 64.5% of the cells underwent apoptosis when the concentration given was 8 μM (Fig. 6B). We further investigated the mechanism involved in the apoptosis induced by compound **1**, and the results showed that with increasing compound **1** concentrations, the cleavage of poly ADP-ribose polymerase 1 (PARP1) protein and caspase 3 concomitantly increased (Fig. 6C), indicating that compound **1** induced apoptosis through a caspase-related mechanism, and thus inhibited the growth of tumor cells.

3.2.3. Compound 1 arrests the cell cycle at the G_1 phase in A431 cells

The effect of compound **1** on the cell cycle distribution of tumor cells was also calculated by staining cells with PI and analyzing with flow cytometry. The result showed that compound **1** treatment arrested

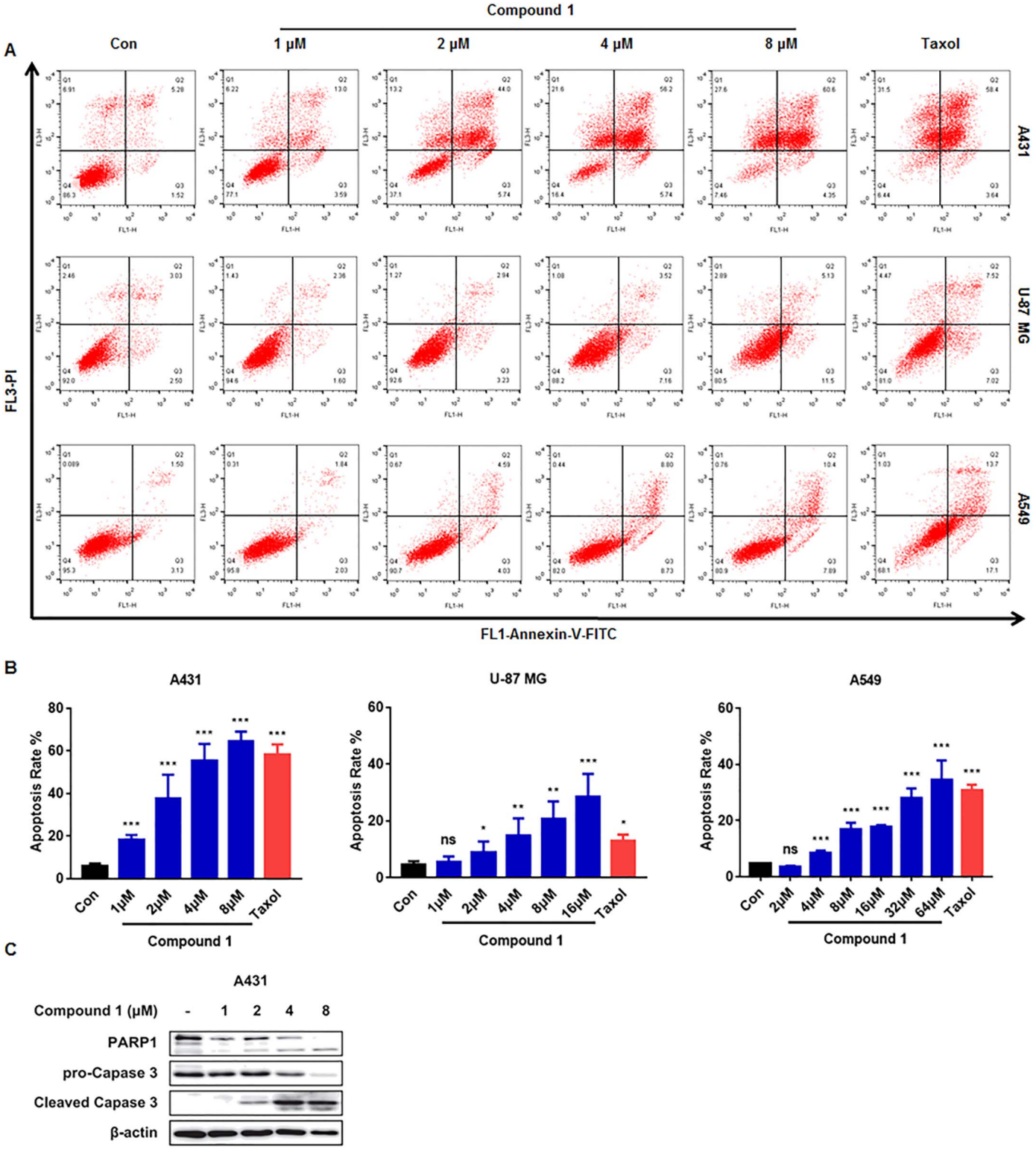

Fig. 6. Compound **1** induces apoptosis of human cancer cells. (A) Compound **1** significantly upregulated the early and late apoptotic levels of A431, U-87 MG and A549 cancer cells, respectively. (B) Apoptosis rates were quantitatively depicted. Statistically significant differences are presented as $^{*}p < 0.05$, $^{**}p < 0.01$, $^{***}p < 0.001$, compared with the control group. ns, not significant. (C) The expression of cleaved PARP1 and caspase 3 in A431 cells treated with compound **1** for 48 h was determined by Western blot analysis.

A431 and A549 cells at the G_1 phase in a dose-dependent manner (Fig. 7A and B). Specifically, exposure to 8 μM compound **1** caused 75.2% of A431 cells and 64.5% of A549 cells occupying the G_1 phase, compared with 39.7% and 47.9% in untreated control cells, respectively. In agreement with these results, the expression of the markers of G_1 phase in A431 cells was modulated by compound **1** treatment. As shown in Fig. 7C, the expression of p-Rb, Cyclin D1, and CDK6 was markedly decreased and the levels of p21 was elevated. Collectively, the results indicate that compound **1** exhibited antitumor effects through arresting tumor cells at the G_1 phase and inducing apoptosis.

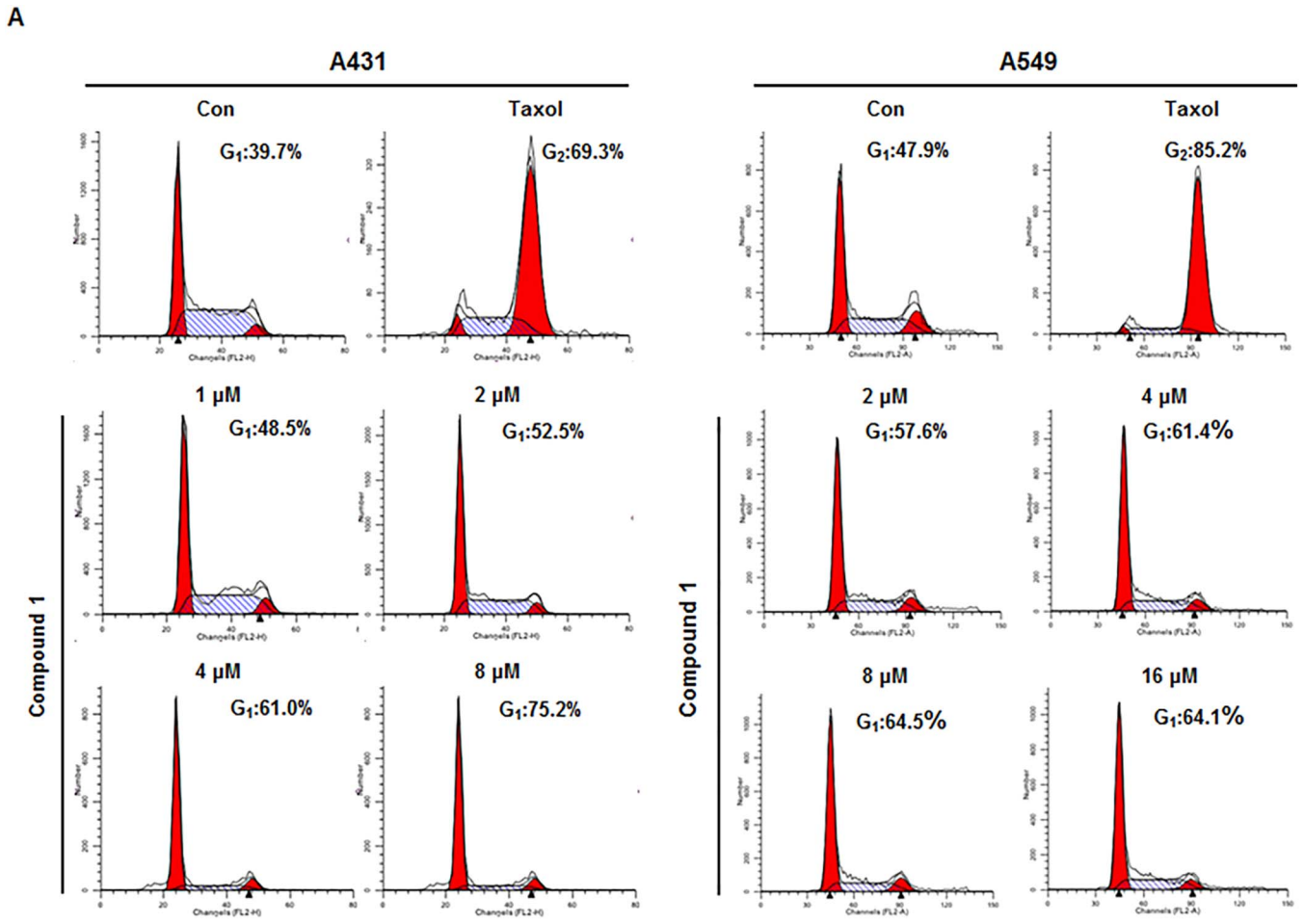

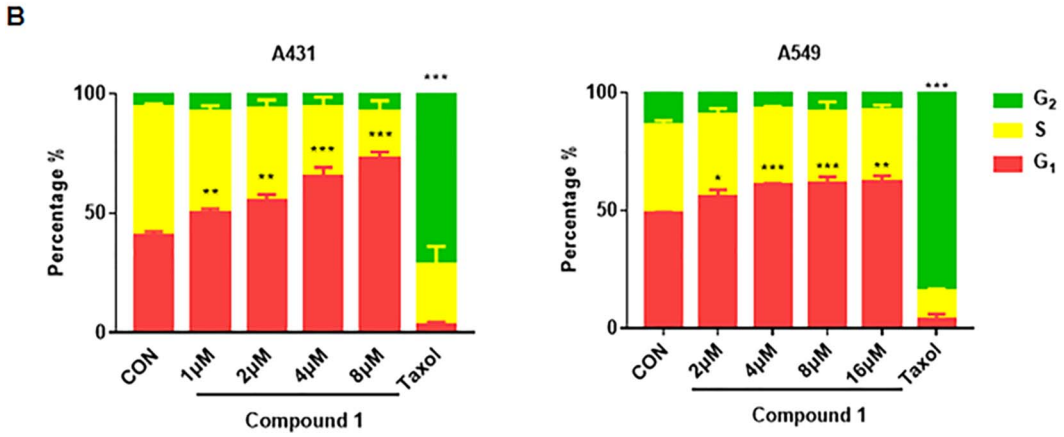

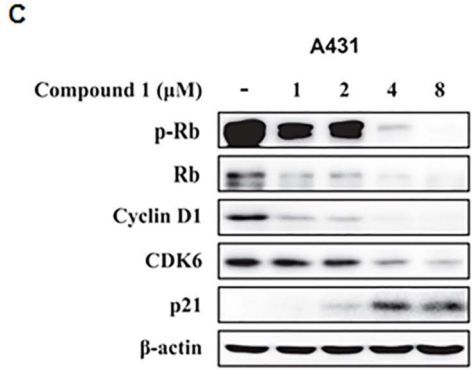

(caption on next page)

Fig. 7. Effects of compound **1** on cell cycle distribution in A431 and A549 cells (A and B). A431 and A549 cells were treated with indicated concentrations of compound **1** for 24 h and the cell cycle distribution were determined by staining with PI. $^{*}p < 0.05$, $^{**}p < 0.01$, $^{***}p < 0.001$, (C) Alterations of G_1 phage related protein expression pattern incubated with compound **1** compared to the cells with vehicle control. A431 cells were treated with compound **1** for 24 h, and the total cell lysates were analyzed by Western blot analysis.

4. Conclusion

In summary, eight new type B nagilactones (**1–8**) and two known analogs (**9–10**) were characterized from the twigs of *P. nagi*. The absolute configurations of compounds **1–3** were confirmed by single crystal X-ray crystallographic analysis using anomalous scattering of Cu Kα radiation. Compounds **3–8** were rare glycosylated nagilactones, especially compounds **3**, **5**, **7** and **8**, which are firstly reported C-17 glycosylated compounds. These findings further enriched the structural diversity of the secondary metabolites in the Podocarpaceae family. Moreover, the cytotoxic evaluation of the isolates against A431, U-87 MG and A549 cell lines showed the aglycones of nagilactones have remarkable cytotoxic activity, especially compound **1**, while the glycosylated nagilactones were inactive. Further studies showed that compound **1** might induce the cell to death *via* triggering apoptosis or arresting cell cycle at the G_1 phase. These results indicated that type B nagilactones may have the potential to be lead compounds fighting against cancer.

Conflict of interest

The authors declare no competing financial interest.

Acknowledgements

The authors thank Mr. Zai-Yong Zhang of Pharmaceutical Analytical & Solid-State Chemistry Research Center of Shanghai Institute of Materia Medica, Chinese Academy of Sciences for his analysis of the crystal structures. Financial support from the Institutes for drug discovery and development (CASIMM0120164010), the Strategic Pilot Projects (XDA12040318), and the Chinese Academy of Sciences (GJHZ1678, GJHZ1739) are greatly acknowledged.

Appendix A. Supplementary data

Supplementary data to this article can be found online at https://doi.org/10.1016/j.fitote.2018.01.007.

References

[1] P. Vineis, C.P. Wild, Global cancer patterns: causes and prevention, Lancet 383 (2014) 549–557.
[2] W. Chen, R. Zheng, P.D. Baade, S. Zhang, H. Zeng, F. Bray, A. Jamal, J. He, Cancer statistics in China, 2016, CA-Cancer J. Clin. 66 (2016) 115–132.
[3] Y. Luo, R.E. Cobb, H. Zhao, Recent advances in natural product discovery, Curr. Opin. Biotechnol. 30 (2014) 230–237.
[4] D.J. Newman, G.M. Cragg, Natural products as sources of new drugs from 1981 to 2014, J. Nat. Prod. 79 (2016) 629–661.
[5] K.H. Altmann, J. Gertsch, Anticancer drugs from nature-natural products as a unique source of new microtubule-stabilizing agents, Nat. Prod. Rep. 24 (2007) 327–357.
[6] A.L. Harvey, Natural products in drug discovery, Drug Discov. Today 13 (2008) 894–901.
[7] T.F. Molinski, D.S. Dalisay, S.L. Lievens, J.P. Saludes, Drug development from marine natural products, Nat. Rev. Drug Discov. 8 (2009) 69–85.
[8] A.F. Barrero, J.F.Q. Del Moral, M.M. Herrador, A convenient synthesis of a-ring-functionalized podolactones. Revision of the structure of wentilactone B, Org. Lett. 4 (2002) 1379–1382.
[9] A.F. Barrero, J.F.Q. Del Moral, M.M. Herrador, Podolactones: a group of biologically active norditerpenoids, Stud. Nat. Prod. Chem. 28 (2003) 453–516.
[10] S. Hanessian, N. Boyer, G.J. Reddy, Total synthesis of oidiodendrolides and related Norditerpene Dilactones from a common precursor: metabolites CJ-14,445, LL-Z1271γ, Oidiolactones A, B, C, and D, and Nagilactone F, Org. Lett. 11 (2009) 4640–4643.
[11] Y. Hayashi, T. Matsumoto, M. Uemura, Carbon-13 NMR studies of the biologically active nor-diterpenoid dilactones from *Podocarpus* plants, Magn. Reson. Chem. 14 (1980) 86–91.
[12] Y. Hayashi, T. Matsumoto, Reaction and interconversion of norditerpenoid dilactones, biologically active principles isolated from *Podocarpus* plants, J. Organomet. Chem. 47 (1982) 3421–3428.
[13] K. Shrestha, A.H. Banskota, S. Kodata, An antiproliferative norditerpene dilactone, Nagilactone C, from *Podocarpus neriifolius*, Phytomedicine 8 (2001) 489–491.
[14] M. Zhang, B. Ying, I. Kubo, Nagilactones from *Podocarpus nagi* and their effects on the feeding and growth of tobacco budworm, J. Nat. Prod. 55 (1992) 1057–1062.
[15] I. Kubo, H. Muroi, M. Himejima, Combination effects of antifungal nagilactones against *Candida albicans* and two other fungi with phenylpropanoids, J. Nat. Prod. 56 (1993) 220–226.
[16] Y.J. Kuo, S.Y. Hwang, M.D. Wu, Cytotoxic constituents from *Podocarpus fasciculus*, Chem. Pharm. Bull. 56 (2008) 585–588.
[17] H.S. Abdillahi, L. Verschaeve, J.F. Finnie, Mutagenicity, antimutagenicity and cytotoxicity evaluation of South African *Podocarpus* species, J. Ethnopharmacol. 139 (2012) 728–738.
[18] Y. Gui, S. Yao, H. Yan, L. Hu, C.Y. Yu, F. Gao, C. Xi, H.H. Li, Y. Ye, Y.P. Wang, A novel small molecule liver X receptor transcriptional regulator, nagilactone B, suppresses atherosclerosis in apoE-deficient mice, Cardiovasc. Res. 112 (2016) 502–514.
[19] K. Sato, Y. Inaba, H.S. Park, Cytotoxic bisnor- and norditerpene dilactones having 7α,8α-epoxy-9,11-enolide substructure from *Podocarpus macrophyllus* D. DON, Chem. Pharm. Bull. 57 (2009) 668–679.
[20] K.P. Devkota, R. Ratnayake, N.H. Colburn, Inhibitors of the oncogenic transcription factor AP-1 from *Podocarpus latifolius*, J. Nat. Prod. 74 (2011) 374–377.
[21] A. Farjon, In a Handbook of the World's Conifer, Brill, Leiden, Netherlands, 2010.
[22] H.S. Abdillahi, J.F. Finnie, J. Van Staden, Anti-inflammatory, antioxidant, anti-tyrosinase and phenolic contents of four *Podocarpus* species used in traditional medicine in South Africa, J. Ethnopharmacol. 136 (2011) 496–503.
[23] Y. Zhang, C.P. Tang, C.Q. Ke, Y. Ye, New cyclopeptide from Podocarpus nagi, Chin. J. Chem. 30 (2012) 1361–1364.
[24] Y.D. Zheng, X.C. Guan, D. Li, L.G. Lin, Y. Ye, Novel diterpenoids from the twigs of *Podocarpus nagi*, Molecules 21 (2016) 1282–1290.
[25] Z.L. Feng, L.L. Zhang, Y.D. Zheng, L.G. Lin, Norditerpenoids and dinorditerpenoids from the seeds of *Podocarpus nagi* as cytotoxic agents and autophagy inducers, J. Nat. Prod. 80 (2017) 2110–2117.
[26] Y. Hao, X. Wang, T. Zhang, D. Sun, Y. Tong, Y. Xu, H. Chen, L. Tong, L. Zhu, Z. Zhao, Z. Chen, J. Ding, H. Xie, H. Li, Discovery and structural optimization of N5-substituted 6,7-dioxo-6,7-dihydropteridines as potent and selective epidermal growth factor receptor (EGFR) inhibitors against L858R/T790M resistance mutation, J. Med. Chem. 59 (2016) 7111–7124.
[27] S.J. Bloor, B.P.J. Molloy, Cytotoxic norditerpene lactones from *Ileostylus micranthus*, J. Nat. Prod. 54 (1991) 1326–1330.
[28] I. Kubo, B.P. Ying, Two nor-diterpene dilactones from *Podocarpus nagi*, Phytochemistry 30 (1991) 1967–1969.
[29] T. Tanaka, T. Nakashima, T. Ueda, Facile discrimination of aldose enantiomers by reversed-phase HPLC, Chem. Pharm. Bull. 55 (2007) 899–901.
[30] D.M. Tian, H.Y. Cheng, M.M. Jiang, Cardiac glycosides from the seeds of *Thevetia peruviana*, J. Nat. Prod. 79 (2015) 38–50.
[31] S.K. Arora, R.B. Bates, P.C.C. Chou, Structures of norditerpene lactones from *Podocarpus* species, J. Organomet. Chem. 41 (1976) 2458–2461.
[32] B. Ying, I. Kubo, T. Matsumoto, Congeners of norditerpene dilactones from *Podocarpus nagi*, Phytochemistry 29 (1990) 3953–3955.
[33] D.J. Newman, G.M. Cragg, Natural products as sources of new drugs over the last 25 years, J. Nat. Prod. 70 (2007) 461–477.
[34] M.A. Jordan, L. Wilson, Microtubules as a target for anticancer drugs, Nat. Rev. Cancer 4 (2004) 253–265.
[35] S.M.A. Hussaini, P. Yedla, K.S. Babu, T.B. Shaik, G.K. Chityal, A. Kamal, Synthesis and biological evaluation of 1,2,3-triazole tethered pyrazoline and chalcone derivatives, Chem. Biol. Drug Des. 88 (2016) 97–109.
[36] X.H. Zhang, J.Y. Shin, J.O. Kim, J.E. Oh, S.A. Yoon, C.K. Jung, J.H. Kang, Synergistic antitumor efficacy of sequentially combined paclitaxel with sorafenib *in vitro* and *in vivo* NSCLC models harboring KRAS or BRAF mutations, Cancer Lett. 322 (2012) 213–222.
[37] Y. Yu, S. Gaillard, J.M. Phillip, T.C. Huang, S.M. Pinto, N.G. Tessarollo, Z. Zhang, A. Pandey, D. Wirtz, A. Ayhan, B. Davidson, T.L. Wang, Inhibition of spleen tyrosine kinase potentiates paclitaxel-induced cytotoxicity in ovarian cancer cells by stabilizing microtubules, Cancer Cell 28 (2015) 82–96.